Study of the e2v ccd 250 : PSF and pixels response sensitivity to light intensity

Pierre Astier, Augustin Guyonnet, Nicolas Regnault, Sylvain Baumont, Pierre Antilogus, LPNHE (Paris)[1]

Abstract

We report analyses carried out on test data of the e2v ccd 250, candidates as LSST sensors. The test data was acquired by Peter Doherty in Harvard during December 2012 on the e2v ccd 250 with the serial number 110-07. We study here the response to flatfields and to spot illuminations. We find two intriguing and perhaps related phenomena: that spots tend to be slightly broader with increasing brightness, and that adjacent pixels in flat-field exhibit positive correlations coefficients, linearly increasing with light level. These two phenomena might share a common cause, but cannot be both entirely explained by this unknown cause: the spot size increase with flux is essentially isotropic, while the neighbor correlations are highly anisotropic.

Contents

February 6, 2013

1. Introduction

The analysis presented here was carried out on test frames acquired by Peter Doherty in Harvard. Those test frames consist in two experimental setups: flat field illuminations and single spot illumination .

The first dataset (dated from Dec. 20-29, 2012) consists in flat field illumination with increasing integrated flux. Those illumination ramps split in two datasets : one with different parallel clock voltage settings, (low level at 0V and high level from +8V to +12V with =1V steps), the other with different illumination wavelengths (500 nm, 700 nm, 900 nm) and parallel clocks from 0 to +10V . All ramps extend up to saturation, meaning different ramps have different maximum exposure time, depending on lamp light yield and CCD efficiency.

The second dataset consists in spots at 2 wavelengths (550 and 900 nm), with parallel clocks from 0 to +10V and increasing integrated flux, obtained by increasing exposure time at fixed spot intensity. The frames are dated from Dec. 21-23, 2012. The spot size is typically $\sim$ 5 pixels FWHM, surrounded by diffraction rings. The data allows one to test for the stability of the spot shape with integrated flux, and in principle for the linearity of the measured flux with the delivered one. This spot series does not go far beyond saturation. This spot data could have been used to assess the linearity of flux measurements. Unfortunately, we can suspect that the lamp intensity varies with time, and the data from the monitoring photodiode was not recorded. This linearity study then has to be postponed.

2. Flat field : study of pixels spatial correlation

CCD device readout is splitted between 16 amplifiers, each reading a 542 by 2022 pixels area. Amplifiers (#9, #10, #11, #12, #13, #14) being noisier than the others, they are not considered for this study.

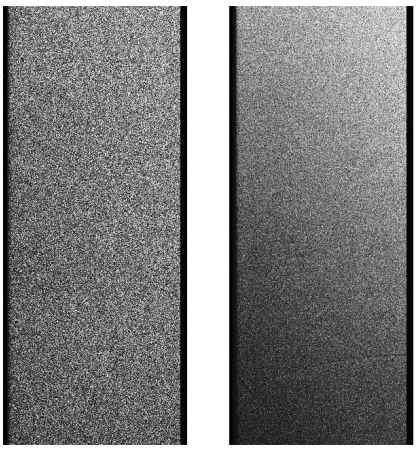

Figure 1: Left : 10 s exposure time of CCD chip 8. Right : 810 s exposure time of CCD chip 8. A vertical gradient in the illumination intensity is visible, as well as a horizontal darker line at the bottom of the image.

2.1. Spatial correlation function

Pixels spatial correlation are measured with the following function :

$$R(k,l) = \frac{\left(\frac{\sum_{i=0,j=0}^{I-k,J-l} (pix_{i,j} - \mu) \times (pix_{i+k,j+l} - \mu)}{(I-k) \times (J-l)} \right)}{\sigma^2}$$

where μ and σ^2 are respectively average and variance of the flux measurement on a given chip. Chip's area is (I, J), minus (k, l), where k and l are the extent in horizontal and vertical direction to which correlations are computed. By definition, $R(0, 0)$ value is 1.

This study is investigating two parameters that might influence pixels correlations in flat field images : the first parameter is clocking voltage value (from 8V to 12V with 1V steps) while the second one is illumination wavelength (500 nm, 700 nm, 900 nm). For each configuration, the dataset consists in a ramp of increasing exposure times, up to saturation.

2.2. Evolution of spatial correlation with respect to voltage value

For each voltage value, a ramp of exposure times is performed from 0 s to 810 s with 10 s steps. Average intensity of the source fluctuates at the

Table 1: Correlations amplifier 8, clocking voltage 9V, 12.5s exposure time (giving Φ = 25140 ADU).

	x	x+1	x+2	x+3
y	1	0.0096	0.0033	0.0008
y+1	0.0342	0.0081	0.0020	-0.0013
y+2	0.0032	0.0036	0.0003	-0.0002
y+3	0.0009	0.0004	0.0038	0.0008

per mil level from one image to the next. This intensity fluctuation does not affect illumination pattern and the difference between two images is flat below 0.01%.

For a single image, pixels exhibit various correlation patterns. They originate in illumination gradient (for instance, figure 1, right), electronic instabilities, or pixel size variations. Subtraction of a pair of flat field exposures is therefore needed to remove contributions other than shot noise to the spatial variation of illumination. The whole correlation analysis is then performed on subtractions of images pairs, and we ignore pixels on difference image whose value is beyond 5 σ of the spatial variations. This is done to remove cosmics which slightly bias measurements. This cut has no effect on the trend of correlations evolution with fluxes, it simply reduces dispersion. Correlations are studied on a subset of images below saturation, that is, approximately below 25 000 ADU (figure 2).

All ramps exhibit a correlation raising with exposure level, in both vertical and horizontal direction[1] with increasing fluxes (figures 3 and 4). It must be noted that slope of correlations $R(0,1)$ decreases with increasing voltage value (figure 5) while the other $R(k,l)$ correlations remain at the same level when clocking voltages are changed (figure 6). Evaluating of $R(k,l)$ slopes for ramps at 11V and 12V is not possible because they are too noisy.

A typical set of $R(k,l)$ values are shown table 1. $R(0,1)$ is approximately four times bigger than $R(1,0)$ while ($R(0,2)$, $R(2,0)$) and ($R(0,3)$, $R(3,0)$) are of the same order.

[1]Vertical direction corresponds to y axis (2022 pixels) in the ds9 display of a chip (x axis (542 pixels) is horizontal direction).

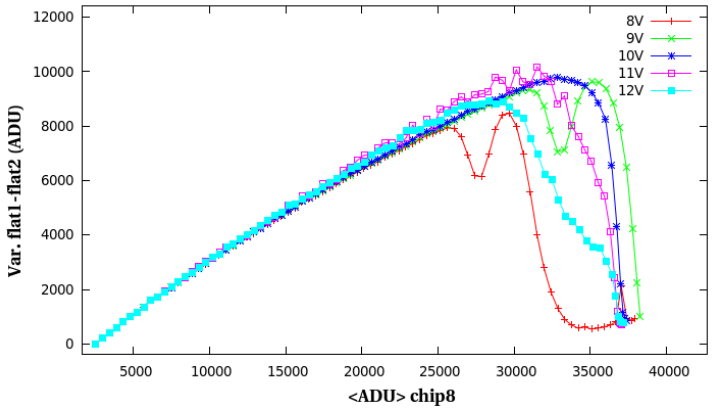

Figure 2: Variances from subtracted pairs of images versus mean flux for a ramp of exposure time and different voltage values.

2.3. Evolution of spatial correlation with respect to illumination color

Dependencies of spatial correlations with respect to flat field color (500 nm, 700 nm, 900 nm) are summarized on figure 7 : it can be seen that evolution of spatial correlations does not change with flat field wavelength, neither in horizontal direction, nor in vertical. Linear fit of vertical +1 pixel correlations between (5000 ADU, 25 000 ADU) gives slopes:
$1.39 \pm 0.04 \times 10^{-6}$ (frac. of variance/ ADU), for 500 nm wavelength,
$1.39 \pm 0.04 \times 10^{-6}$ (frac. of variance/ ADU), for 700 nm wavelength,
$1.42 \pm 0.03 \times 10^{-6}$ (frac. of variance/ ADU), for 900 nm wavelength.
Spatial correlations do not seem to depend on illumination wavelength.

At a given flux, it must be pointed out that varying exposure time has no effect on correlation evolution : 700 nm illumination ramp extend from 0 s to 60 s while 500 nm ramp goes up to 180 s, but they both exhibit the same correlation slope with respect to flux.

2.4. Checking for influence of parallel shifts

One might suspect that correlations are influenced by parallel shifts. To investigate that, we analyze separately the first (pixels $0<j<1012$) and second halves of the chip (pixels $1012 \leq j<2022$). The result is shown on figure 8 : correlations evolve the same pace for both halves. In fact, even a finer slicing does not reveal differences: correlations do not depend on line number.

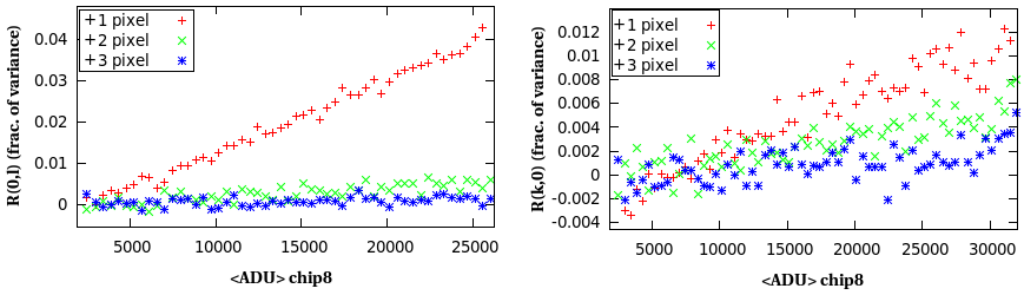

Figure 3: 8V dataset : vertical pixels correlations are represented on left plot while horizontal pixels correlations are shown on right plot : vertical correlations are approximately 4 times higher than horizontal ones. Small correlations still exist at +2 pixels (see next figure).

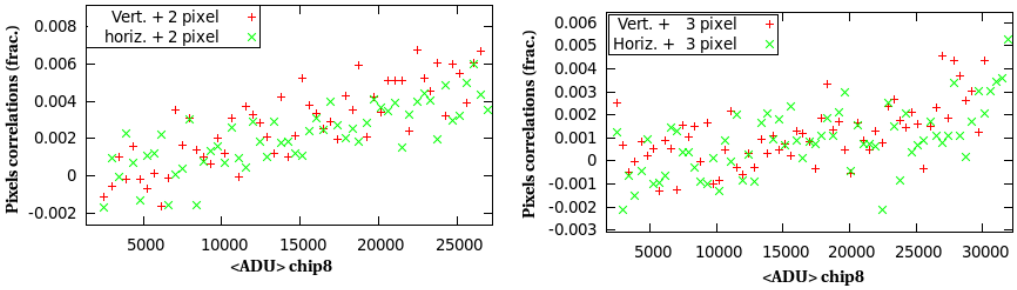

Figure 4: Comparison of long range vertical and horizontal correlation. At +2 pixels, as well as at +3 pixels, correlations are similar in the vertical and horizontal direction. At +2 pixels, they are approximately equal to 0.6% at a flux of 30 000 ADU, while they are approximately equal to 0.3% at +3 pixels.

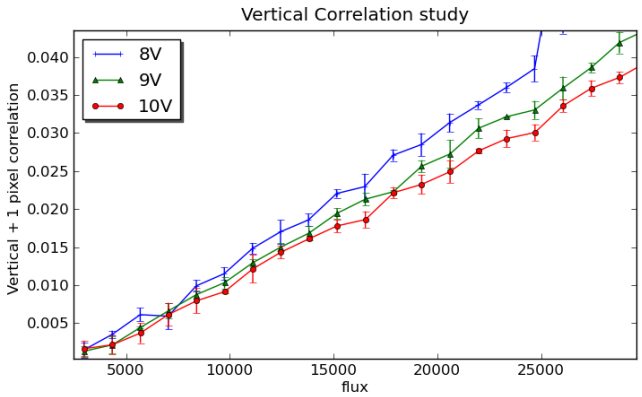

Figure 5: Comparison of evolution of vertical +1 correlations for different voltage values (amplifier 8). Slopes of pixels correlations with respect to flux is decreasing with increasing voltage values. This trend is also visible on the other amplifiers.

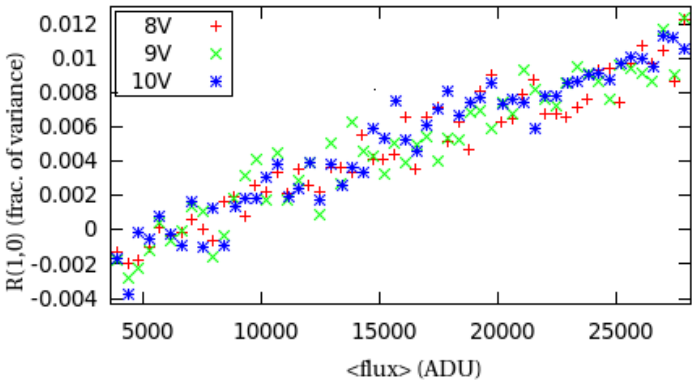

Figure 6: Comparison of evolution of horizontal +1 correlations for different voltage values (amplifier 8). In this direction, slopes of pixels correlations with respect to flux is independant of voltage.

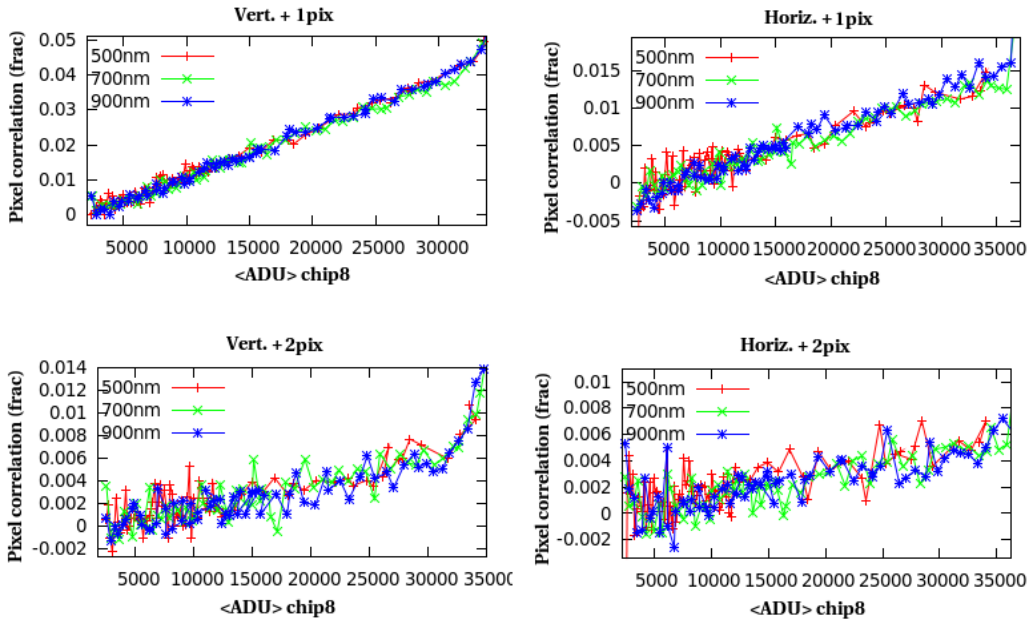

Figure 7: Evolution of spatial correlations with respect to flux for different flat field color (500 nm (red), 700 nm (green), 900 nm (blue) : correlations amplitude do not seem to depend on illumination wavelength.

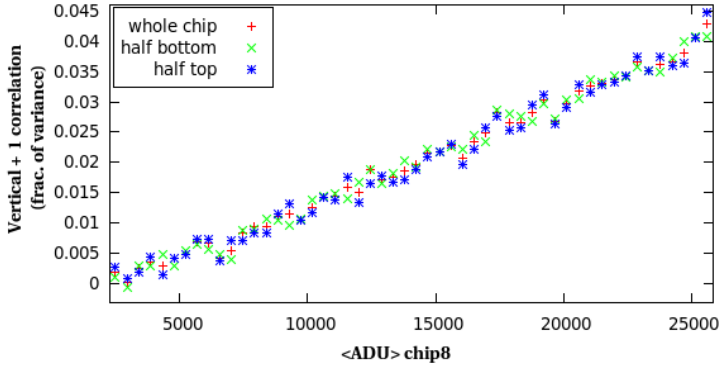

Figure 8: Comparison of vertical +1 pixel correlation evolution with respect to flux for two distinct part of a chip : half bottom in green ($0<j<1012$) and half top in blue ($1012 \leq j < 2022$). Those two areas show the same correlation evolution.

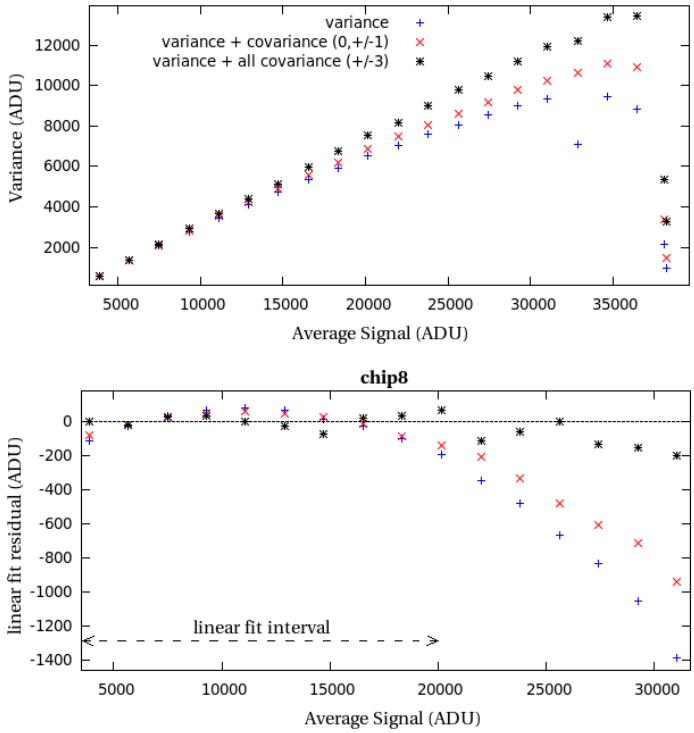

Figure 9: top : PTC of amplifier 8, clocking voltage +9V : assuming no pixel correlation (blue), taking into account the dominant correlation, vertical +/-1 (in red), adding covariances up to +3 pixels in all directions. Bottom : linear fit residuals for each case (fit is performed below 20 000 ADU). When covariances are accounted for in the PTC relation, linearity is restored up to higher fluxes.

2.5. PTC taking covariance into account

Linearity of PTC relation can be greatly improved when taking into account pixels correlation. This is done adding covariances up to 3 pixel distance in all directions. Improvement of PTC linearity is visible on figure 9: linearity is restored up to 30 000 ADU. Though, it must be noticed that residuals are significantly scattered.

3. Study of spot sizes

3.1. Methods

We first extract the fits image extension 4 that contains the spot and subtract a master bias, aligned on the image overscan (chosen as `[524:542,1:2000]`).

We then checked that the image level is spatially flat and close to 0. Since we used medians both when building the master bias, and when ajusting it to the image level, the resulting images are affected by more quantization noise than ultimately achievable. Since these images have a gain of about 5 e/ADU, a detailed analysis of flux linearity would deserve a better handling of bias.

We have then carried out a number of measurements on the resulting images: the spot size and position, the aperture flux, and the flux in an aperture of same size but away from the spot. For the spot position and size, we used weighted first and second moments. Namely, we use a Gaussian weight and adjust its size so that the measured weighted second moments are half the ones of the weighting function: in this way the object contributes as much as the weight. In practice, we iteratively solve for the matrix of second moments $\boldsymbol{M}_g$ until it satisfies:

$$\boldsymbol{M}_g = 2\frac{\sum_{pixels}(\boldsymbol{x}_i - \boldsymbol{x}_c)(\boldsymbol{x}_i - \boldsymbol{x}_c)^T e^{-\frac{1}{2}(\boldsymbol{x}_i-\boldsymbol{x}_c)^T {\boldsymbol{M}_g}^{-1}(\boldsymbol{x}_i-\boldsymbol{x}_c)} I_i}{\sum_{pixels} e^{-\frac{1}{2}(\boldsymbol{x}_i-\boldsymbol{x}_c)^T {\boldsymbol{M}_g}^{-1}(\boldsymbol{x}_i-\boldsymbol{x}_c)} I_i} \qquad (1)$$

where $\boldsymbol{x}_i$ are pixel coordinates, $\boldsymbol{x}_c$ the Gaussian weighted centroid, and I_i is the (sky subtracted) image value at pixel i. The position $\boldsymbol{x}_c$ is obtained using the same iterations. This algorithm performs well on real astronomical images, where it can be used to extract stars by the similarity of their second moments.

Any measurement of second moments on noisy images has to rely on some sort of weighting function, because the unweighted second moment expression does not have a finite variance. Since any weighting function will unavoidably introduce a length scale, we devised the above scheme where this scale is dictated by the object being measured. Typical alternatives consist in integrating the second moments up to a certain S/N of pixels, but the result then depends on the object S/N. Note that our approach is insensitive to S/N on average, since the image noise does not enter into the calculation, and we checked on simulations of non-Gaussian spots that the recovered average sizes are indeed insensitive to S/N.

These size estimators are not faithful estimators of the actual second moments: since spots (or stars) tend to exhibit wings brighter than expected for Gaussian shapes, the second moments we compute are typically underestimated, but in reproducible way. Most of the image quality estimators have their own peculiarities, and should only be used to compare spot sizes of similar shapes.

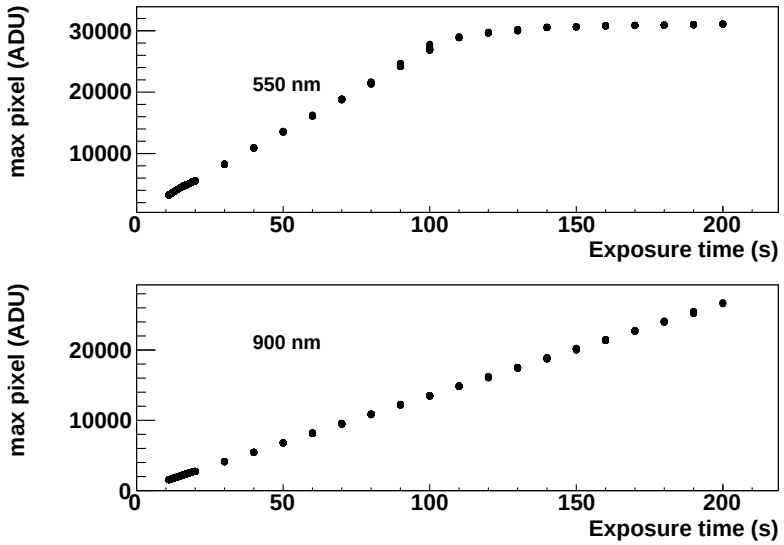

Figure 10: Maximum spot pixel value as function of exposure time. Saturation occurs at 100 s at 550 nm, and is not reached for 200 s at 900 nm.

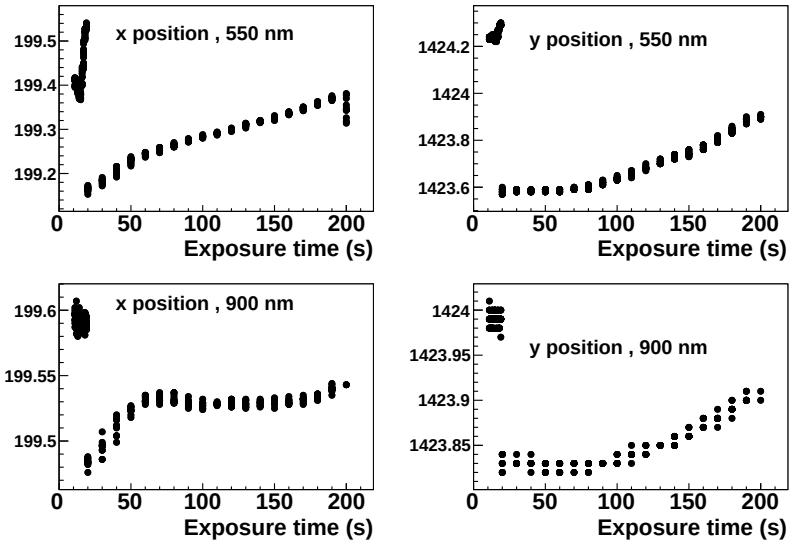

Figure 11: Measured plot positions (in pixels) as a function of exposure time for the two sets of measurements. The small exposure times belong to a different sequence than the remainder. The position drifts by fractions of a μm, which seems very difficult to avoid.

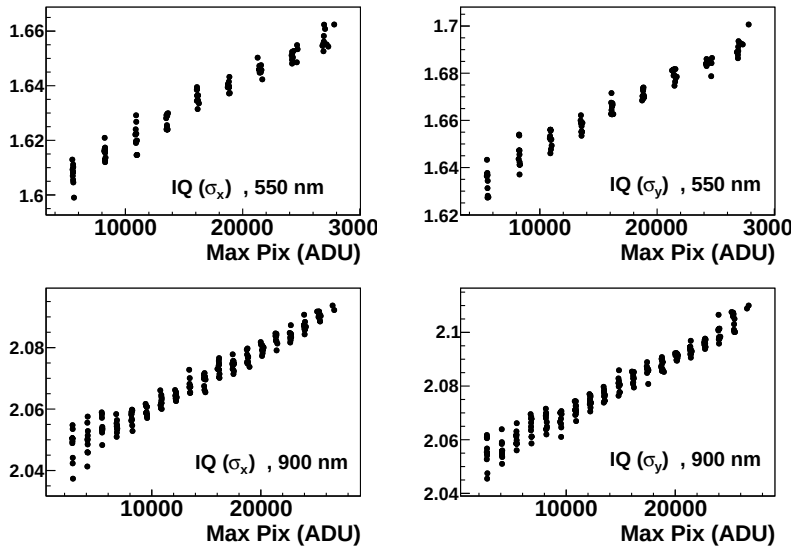

Figure 12: Measured plot sizes (r.m.s in pixels) as a function of spot peak flux at two wavelengths. One notes that the size seems to slowly increase with the peak flux.

3.2. Results

The spot series we have in hand has integration times ranging from 1 to 200 s. On figure 10, one can see that the saturation occurs at 100s at 550 nm, while the 200s images are unsaturated at 900 nm.

We soon realized that the spot position slightly moves between successive exposures. Figure 11 displays the spot position indexed by exposure time. The small drifts are much below 1 μm and are not unexpected. The spots at low exposure time exhibit different positions because they were acquired as an other sequence. We hence did not compare those to the higher exposure times.

The r.m.s spot sizes along x and y (defined by equation 1) are displayed in figure 12 as a function of peak flux. They seem to increase with spot flux in both directions and at both wavelengths. Before discussing the details of the result, we first argue that the effect is not an artifact of our spot size measurement technique.

First, we have mentioned that on simulations of non Gaussian spots of identical shapes but varying S/N ratios, our second moment estimator is independent on average of S/N. Second, the ratio $f_{peak}/flux$ constitutes a rudimentary spot size indicator, and figure 13 confirms the trend displayed

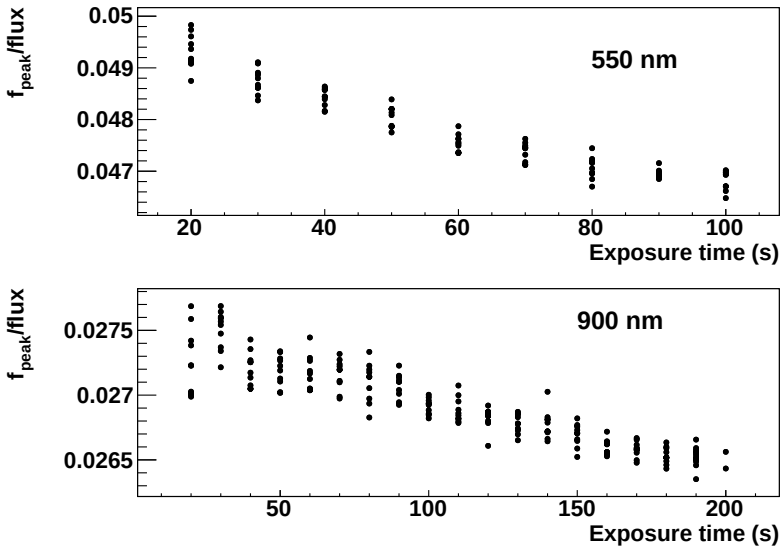

Figure 13: Peak pixel value divided by aperture flux (50 pixels diameter) as a function of exposure time. The tendency of spots getting broader with integrated flux is visible, and supports figure 12.

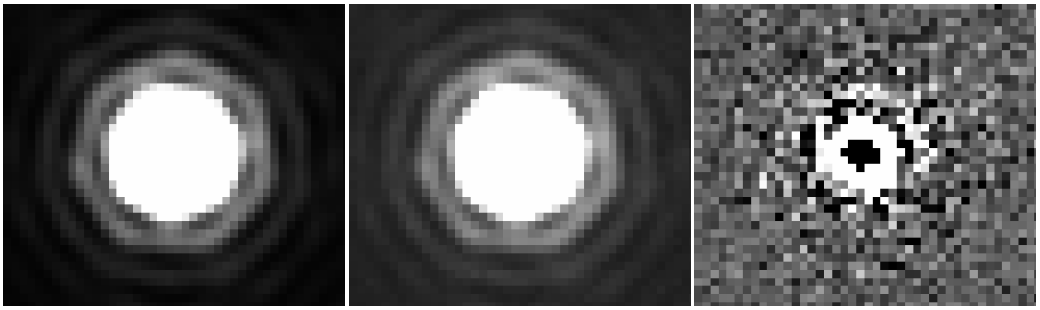

Figure 14: Difference of a 200-s spot (900 nm) from a sum of 20-s spots after geometrical alignement via a flux-conserving resampling and proper normalisation to integration times. Left : 200-s spot; middle sum of ten 20-s spots; right : difference. The broader wings and lower peak of the bright spot clearly show up.

on figure 12.

One can also visualise the different shapes of spots by image subtraction. The small position shifts impose to resample spots prior to subtraction. We resampled both 200-s and 20-s spots (at 900 nm) to bring them into spatial coincidence (using our Gaussian weighted position estimators), and subtracted after flux scaling from exposure times. The stronger wings and weaker core of the 200-s spot are clearly visible on the subtraction (figure 14).

4. Discussion and Conclusion

The fact that at high flux, the photon transfert curve (see figure 2) shows a variance lower that the flux mean, has been observed in many optical CCD and has been already attributed in some papers to increasing measured flux correlation between nearby pixels with the amount of collected charge (see for example [1]). In the same way, our study on the e2v CCD 250 based on flat differences, shows a linear increase of a postive correlation in the measured flux for nearby pixels. In our case this correlation appears to be similar in the serial (x) and parallel directions at large scale (+/-2 and +/-3 pixels), but highly asymetric for the closest pixels (+/-1 pixels) : the correlation being $\sim$4 time higher allong the parallel direction (up to $\sim$4%) compared to the serial direction.

No significant wavelength dependence of these correlations has been measured, corresponding to a relative change in the correlation between 550 nm and 900 nm below $\sim$5% . This is a hint that the phenomenon at the origin of these correlations is localized near the e storage area.

The increase of spot size with flux seems to be linear with peak flux and amounts to 2-3 % from a vanishing spot to saturation for our "star like" spots. The fact that the relative measured growth is smaller at 900 nm than at 550 nm might be related to the red spot being naturally broader in a first place, due to diffraction in the illuminating set-up. We observe a marginally larger increase (by 10-20%) of the spot size along columns compared to along rows.

We tried to find evidence of the same phenomenon on other CCDs. We successfully detect it on astronomical images from both Megacam[2] (on

[2] CCD42-90 from e2v: pixel size 13.5x13.5 micron, 3 phases, blue-sensitive back-illuminated thinned devices (e2V data sheet) Full $\sim$ 150 ke$^-$, but limited by readout saturation which occurs first, and hence unchecked.

CFHT), and DECam[3] (on CTIO), with different amplitudes. We observed a 0.5% size increases from a vanishing star to saturation in Megacam data, and a slightly bigger effect in DECam data. Broadly speaking, the phenomenon seems fairly achromatic and the relative increase rate of star sizes with flux gets shallower when image quality (seeing) degrades, as seen in our spot studies with LSST sensors. In this on-sky data, we find that the increase rates are similar along rows and columns, with a mild indication that it might be slightly larger (10 to 20 %) along columns.

Transfers between adjacent pixels depending on the pixels' contents make physical sense (basically, electrons repel each other), and we are currently quantifying the observed phenomenon using this simplistic ansatz. Simulations deliver the linear increase of spot size we observe, together with a lower impact for poorer image qualities. This simple model also delivers positive correlations of neighbor pixels in flatfield images, linearly increasing with illumination level, as we observe. We are however puzzled by the clear anisotropy of the correlations seen at ± 1 pixels in the flats, difficult to accomodate with the observed quasi-isotropy of the spot size increase.

References

[1] M. et. al. Downing. CCD riddle: a) signal vs time: linear; b) signal vs variance: non-linear. *Proc SPIE*, pages 6276–09, 2006.

[3] LBL CCD: pixels size 15x15 microns, 3 phases , red-sensitive 250 μm thick, fully depleted, back-illuminated devices. Full well > 130 ke$^-$